19. CHEMISTRY OF LEG 45 BASALTS

J. M. Rhodes,[1] D. P. Blanchard,[3] M. A. Dungan,[4] K. V. Rodgers,[2] and J. C. Brannon[2]

INTRODUCTION

A total of 764 meters of volcanic basement was sampled during Leg 45 at Sites 395 and 396; most of the material recovered consists of basaltic pillow lavas, thin flows, and more massive cooling units. This paper is concerned with the major-and trace-element chemistry of these basalts. A companion paper by Dungan et al. (this volume) discusses the petrography, mineral chemistry, and 1-atmosphere melting experiments for the same suite of samples. The emphasis here will be on samples recovered from Holes 395 and 395A. Data for samples from Hole 396 are included for completeness, but will be reported in detail, together with data on samples from Hole 396B, in the Leg 46 *Initial Reports.*

Major- and trace-element analyses for 59 basalt samples from Holes 395 and 395A are given in Table 1; analyses for 8 samples from Hole 396 are given in Table 2. In these tables, the samples are listed in order of increasing depth within basement, reported to the nearest meter. Also indicated in Tables 1 and 2 are the major magmatic compositional units, first identified on the basis of shipboard X-ray fluorescence analyses, and modified slightly in the light of the recent data. Within these two tables, the oxidation ratio (O.R.) is given as Fe_2O_3/(total iron as FeO). The atomic ratio Mg/(Mg+Fe) has been calculated, after adjustment for the oxidation state of iron, such that the ratio Fe^{3+}/(Total iron as Fe^{2+}) is 0.1 (Bass, 1971). For convenience, the atomic Mg/(Mg+Fe) ratio is designated the Mg′-value in Tables 1 and 2 and throughout the paper. The same convention for handling the oxidation state of iron has been used in the CIPW norm calculations that are referred to in the text and illustrated in Figure 1.

Table 3 presents additional trace-element data on 26 samples selected from Table 1 on the basis of petrography and major element chemistry.

The major-element data were obtained by X-ray fluorescence analysis (XRF) on fused glass discs, prepared by fusing the sample with a lanthanum-bearing lithium borate fusion mixture (Norrish and Hutton, 1969). FeO was determined titrimetrically using the modified cold acid digestion method of Wilson (Maxwell, 1968), and Fe_2O_3 was obtained by difference from the XRF total iron value. Na_2O was determined on a separate 20 to 30 mg aliquant by instrumental neutron-activation analysis (INAA). Total water content was measured coulometrically using a DuPont moisture analyzer, in which the sample is fused with a lead oxide flux.

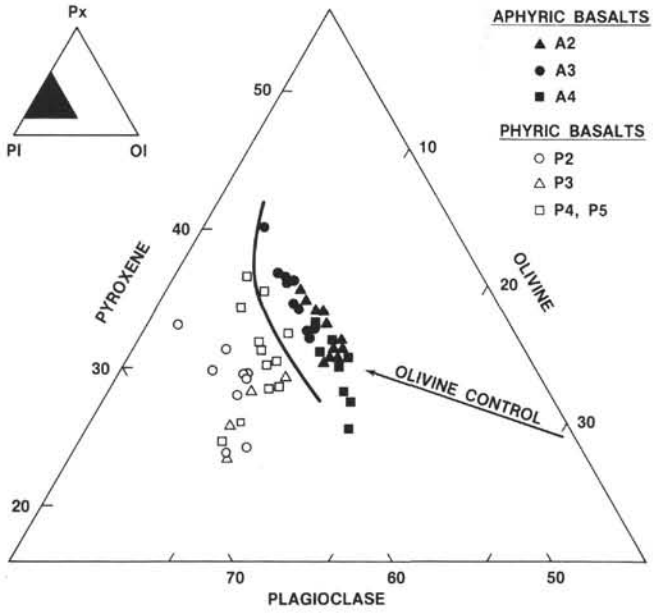

Figure 1. *Normative olivine-plagioclase-pyroxene relationships in Leg 45 basalts. The classification and inferred olivine-plagioclase cotectic is from Shido et al. (1971).*

The trace elements (Rb, Sr, Y, Zr, Nb) were determined by XRF analysis on pressed powder pellets. Corrections were made for non-linear backgrounds, tube contamination, and inter-element interferences (Norrish and Chappell, 1967). Corrections for matrix effects were based on a modification of the Compton scattering method (Reynolds, 1967), using the Ag-Compton peak. Additional trace-element data (Table 3) (La, Ce, Sm, Eu, Tb, Yb, Lu, Hf, Cr, Sc, Ni) were obtained by INAA following the methods of Jacobs et al. (in press).

BASALT CHEMISTRY

All the basalts recovered from Holes 395, 395A, and 396 are olivine and hypersthene normative, containing between 1.8 and 14.2 per cent of normative olivine, and plotting in the olivine tholeiite field of the basalt tetrahedron (Yoder and Tilley, 1962). Alkali basalts and transitional tholeiites are conspicuously absent, as also are quartz tholeiites. They have the overall com-

[1]Lockheed Electronics Co., Inc., Houston, Texas. Present address: Dept. of Geol. and Geog., Univ. of Massachusetts, Amherst.
[2]Lockheed Electronics Co., Inc., Houston, Texas.
[3]NASA, Johnson Space Center, Houston, Texas.
[4]NASA, Research Associate, Johnson Space Center, Houston, Texas.

TABLE 1
Chemical Composition of Basalt From Site 395

Sample (Interval in cm)	395-11-1, 42-44	395-11-1, 136-138	395-11-2, 100-105	395-15-2, 68-72	395-16-2, 63-66
JSC No.	109	110	111	112	113
Depth (m)	93	94	95	133	142
Basalt type	A_2*	A_2*	A_2*	A_2*	A_2*
SiO_2	49.4	49.3	48.5	49.3	49.6
TiO_2	1.62	1.61	1.58	1.60	1.66
Al_2O_3	15.09	14.84	14.79	14.68	15.15
Fe_2O_3	1.28	1.36	1.81	2.61	4.62
FeO	9.83	9.73	9.06	8.33	6.94
MnO	0.20	0.19	0.17	0.18	0.19
MgO	8.51	8.45	8.56	8.40	8.17
CaO	10.41	10.34	10.18	10.17	10.43
Na_2O	2.80	2.92	2.82	2.89	2.82
K_2O	0.11	0.10	0.14	0.14	0.16
P_2O_5	0.13	0.11	0.12	0.13	0.16
S	0.11	0.11	0.11	0.12	0.10
Total H_2O	0.55	0.43	1.56	1.42	0.91
Total	100.04	99.50	99.37	99.94	100.94
Total Fe as FeO	10.98	10.95	10.69	10.68	11.10
Mg′-value	0.605	0.605	0.613	0.609	0.593
O. R.	0.117	0.124	0.169	0.244	0.416
Trace Elements (ppm)					
Rb	1.2	0.9	1.7	1.1	1.1
Sr	115	112	116	116	115
Y	35	35	34	35	37
Zr	105	105	102	106	106
Nb	2.4	1.9	1.9	1.7	1.8

Sample (Interval in cm)	395A-8-1, 70-73	395A-9-1, 73-79	395A-9-2, 100-104	395A-10-1, 144-146	395A-13-1, 142-147
JSC No.	120	121	122	123	124
Depth (m)	126	135	137	145	174
Basalt type	A_2	A_2	A_2	A_2	P_2
SiO_2	48.7	48.5	48.9	48.8	49.2
TiO_2	1.66	1.60	1.63	1.60	1.37
Al_2O_3	15.40	14.69	14.92	14.90	17.34
Fe_2O_3	2.56	2.84	2.67	1.97	2.52
FeO	8.81	8.03	8.20	8.96	5.96
MnO	0.20	0.20	0.19	0.19	0.15
MgO	7.60	8.21	8.15	8.40	6.55
CaO	10.46	10.17	10.29	10.23	11.54
Na_2O	2.90	2.93	3.01	2.90	2.83
K_2O	0.18	0.16	0.15	0.14	0.11
P_2O_5	0.17	0.12	0.13	0.12	0.10
S	0.10	0.14	0.14	0.13	0.09
Total H_2O	1.62	1.93	1.25	1.41	1.94
Total	100.33	99.56	99.61	99.79	99.66
Total Fe as FeO	11.11	10.59	10.60	10.73	8.23
Mg′-value	0.575	0.606	0.604	0.608	0.612
O. R.	0.230	0.269	0.252	0.184	0.306
Trace Elements (ppm)					
Rb	1.6	1.5	1.3	1.3	1.1
Sr	119	118	114	115	153
Y	35	35	36	32	29
Zr	104	103	106	103	94
Nb	2.0	1.7	1.6	2.1	1.7

positional characteristics typical of mid-ocean ridge tholeiites, as is indicated by their relatively constant SiO_2 concentrations and low TiO_2 abundances, together with low total alkali content and K_2O/Na_2O ratios (e.g., Engel et al., 1965; Melson et al., 1976). K_2O abundances are characteristically low in most of the samples (<0.2%), and where comparative data are available, do not differ significantly from the K_2O content of basaltic glass from the same samples. A few samples have higher K_2O contents, not related to

TABLE 1 – *Continued*

395-16-3, 3-8	395-18-2, 43-46	395-19-1, 57-62	395A-4 1, 66-69	395A-5-1, 6-10	395A-6-1, 130-134
114	115	116	117	118	119
143	161	170	98	106	117
A_2*	P_1*	P_2*	A_3	A_2	A_2
48.9	48.8	49.7	49.5	49.2	48.7
1.60	1.14	1.29	1.70	1.63	1.60
14.69	16.67	18.48	15.18	15.11	14.74
2.20	2.90	3.23	2.86	3.95	4.30
8.87	5.90	4.45	7.44	6.04	6.82
0.18	0.15	0.12	0.17	0.17	0.18
8.47	8.07	5.99	7.69	7.74	8.08
10.25	12.24	12.10	11.17	11.03	10.11
2.87	2.34	2.68	2.74	2.79	2.97
0.17	0.13	0.11	0.28	0.26	0.22
0.12	0.09	0.10	0.15	0.17	0.12
0.14	0.05	0.03	0.07	0.05	0.07
1.53	0.89	1.97	1.08	1.51	2.48
99.94	99.38	100.27	100.04	99.64	100.45
10.85	8.51	7.36	10.01	9.60	10.69
0.607	0.653	0.617	0.603	0.615	0.599
0.203	0.341	0.439	0.286	0.411	0.402
1.1	1.5	1.2	2.6	3.3	3.0
118	110	158	131	129	118
36	26	26	36	35	34
108	71	85	119	113	104
2.1	1.1	2.0	2.3	1.9	2.0

395A-14-2, 140-147	395A-14-3, 29-34	395A-15-1, 75-81	395A-15-4, 10-15	395A-15-4, 10-15	395A-15-4, 99-107
125	126	127	128(1)	128(2)	129
185	186	192	196	196	197
P_2	P_2	P_2	P_2	P_2	P_2
49.1	49.7	49.0	49.0	49.5	48.3
1.34	1.33	1.35	1.36	1.35	1.30
17.93	18.13	17.51	17.65	17.57	18.01
1.57	2.40	2.69	1.40	(1.40)	2.34
6.94	5.86	5.97	7.25	7.25	5.96
0.13	0.14	0.13	0.13	0.14	0.15
6.81	6.58	6.97	7.07	7.03	6.82
11.73	11.74	11.54	11.58	11.57	11.51
2.80	2.85	2.76	2.71	(2.71)	2.87
0.09	0.07	0.11	0.11	0.11	0.08
0.10	0.12	0.11	0.12	0.12	0.09
0.10	0.12	0.12	0.11	0.11	0.08
1.48	1.46	1.63	1.71	–	1.65
100.12	100.49	99.87	100.21	–	99.20
8.35	8.02	8.39	8.51	8.52	8.07
0.618	0.619	0.622	0.622	0.620	0.626
0.188	0.299	0.321	0.165	–	0.343
0.9	0.5	1.0	1.3	1.0	0.5
152	152	155	156	152	154
27	27	30	29	29	28
87	86	95	91	93	89
1.2	1.9	1.4	1.4	1.8	1.7

basalt type, which are presumably the result of seawater alteration, although this is not always correlated with total water content or the oxidation ratio.

The minor- and trace-element abundances are, similarly, within the range of typical mid-ocean ridge tholeiites (Kay et al., 1970; Schilling, 1971; Pearce and Cann, 1973; Hart, 1976; Bryan, et al., 1976; Erlank and Kable, 1976). This is illustrated by the chondrite-normalized rare-earth patterns, which range between 13 and 24 times chondritic abundances for Sm, and which

TABLE 1 – *Continued*

Sample (Interval in cm)	395A-15-5, 16-20	395A-17-1, 46-55	395A-19-1, 132-136	395A-21-1, 87-90	395A-23-1, 51-55
JSC No.	130	131	132	133	134
Depth (m)	198	211	231	242	261
Basalt type	P_2	P_3	P_3	P_3	P_4
SiO_2	48.9	48.9	49.1	49.8	49.2
TiO_2	1.14	1.09	1.08	1.03	1.12
Al_2O_3	19.16	18.05	16.85	17.73	18.51
Fe_2O_3	1.47	3.70	3.42	2.58	3.76
FeO	6.19	4.78	4.80	5.23	4.24
MnO	0.13	0.15	0.13	0.14	0.14
MgO	6.96	6.66	7.61	7.53	6.51
CaO	11.83	12.83	12.19	12.49	12.59
Na_2O	2.75	2.50	2.31	2.39	2.75
K_2O	0.07	0.12	0.13	0.15	0.15
P_2O_5	0.09	0.09	0.08	0.10	0.12
S	0.09	0.01	0.01	0.03	0.01
Total H_2O	1.63	1.19	1.94	1.68	1.01
Total	100.41	100.08	99.67	100.91	100.10
Total Fe as FeO	7.51	8.11	7.88	7.55	7.62
Mg'-value	0.647	0.619	0.657	0.664	0.629
O. R.	0.196	0.456	0.434	0.342	0.493
Trace Elements (ppm)					
Rb	0.6	1.9	2.1	1.7	1.4
Sr	153	119	110	112	138
Y	24	24	23	22	24
Zr	76	65	64	60	68
Nb	0.7	0.9	1.2	1.5	1.3

Sample (Interval in cm)	395A-31-1, 96-107	395A-33-1, 142-148	395A-34-1, 140-143	395A-35-1, 26-32	395A-36-1, 46-50
JSC No.	142	143	144	145	146
Depth (m)	337	355	364	373	383
Basalt type	P_5	P_5	A_3	A_3	A_3
SiO_2	49.8	48.9	49.5	49.3	48.9
TiO_2	1.10	1.14	1.69	1.67	1.67
Al_2O_3	18.62	17.55	15.32	1.501	15.13
Fe_2O_3	3.28	4.08	2.98	4.50	4.10
FeO	4.49	4.00	7.24	5.66	5.80
MnO	0.12	0.14	0.19	0.16	0.19
MgO	6.69	7.11	7.61	7.45	7.48
CaO	12.17	11.85	11.21	10.95	11.09
Na_2O	2.89	2.73	2.80	2.88	2.93
K_2O	0.18	0.18	0.22	0.32	0.26
P_2O_5	0.08	0.11	0.17	0.13	0.14
S	0.01	0.01	0.09	0.03	0.02
Total H_2O	1.77	1.86	1.33	1.95	2.28
Total	101.23	99.66	100.32	100.03	100.03
Total Fe as FeO	7.44	7.67	9.92	9.71	9.49
Mg'-value	0.614	0.647	0.603	0.603	0.609
O. R.	0.440	0.532	0.300	0.463	0.432
Trace Elements (ppm)					
Rb	2.6	2.5	1.0	4.7	3.3
Sr	175	151	127	133	130
Y	23	23	36	35	36
Zr	71	73	116	117	117
Nb	0.8	1.0	2.4	2.0	1.9

display the light rare-earth depletion typical of "normal" or type I ocean ridge basalts (Bryan, et al., 1976). Mg'-values in these rocks vary from about 0.57 to 0.67 (Figure 2), which is within the range prevalent for mid-ocean ridge basalts but is lower than the values found in the most primitive basalts so far identified (Frey et al., 1974; Bryan and Moore, 1976; Rhodes et al., in press). These values, together with low Ni concentrations, moderately high magmaphile element abundances, and the presence of multiple phenocryst phases (Dungan et al., this volume), are taken as evidence that these basalts have all undergone a substantial differentiation history.

TABLE 1 – *Continued*

395A-24-2, 69-72	395A-25-1, 96-100	395A-26-2, 125-129	395A-27-2, 111-116	395A-38-1, 105-112	395A-29-1, 125-131
135	136	137	138	139	141
272	280	292	301	309	317
P_4	P_4	P_4	P_4	P_5	P_5
49.1	49.3	38.9	49.6	48.8	49.8
1.15	1.14	1.25	1.14	1.19	1.14
17.26	17.10	18.85	17.13	19.09	17.07
2.80	2.58	3.41	1.94	.307	2.65
5.11	5.28	4.85	6.03	4.97	5.73
0.15	0.14	0.17	0.15	0.15	0.15
7.90	7.67	5.87	8.03	6.33	8.00
12.17	11.99	12.27	12.08	12.22	12.04
2.65	2.62	2.84	2.64	2.78	2.59
0.13	0.14	0.16	0.15	0.15	0.13
0.09	0.11	0.13	0.10	0.11	0.10
0.00	0.01	0.02	0.02	0.02	0.02
0.88	1.54	1.26	0.71	0.97	0.83
99.42	99.58	99.96	99.69	99.87	99.41
7.63	7.60	7.92	7.78	7.73	8.11
0.672	0.667	0.595	0.671	0.619	0.661
0.367	0.339	0.431	0.249	0.397	0.327
1.5	2.3	2.5	2.1	2.7	2.0
131	133	165	129	159	132
25	24	26	25	27	25
72	73	82	73	82	74
1.5	0.9	1.3	1.0	1.1	1.3

395A-38-1, 142-148	395A-41-1, 107-111	395A-46-1, 61-64	395A-49-1, 26-31	395A-50-2, 143-147	395A-51-3, 78-82
147	148	149	150	151	152
393	428	476	504	516	526
A_3	A_3	A_3	A_3	A_3	A_4
48.6	49.7	49.3	49.5	48.8	48.8
1.65	1.70	1.75	1.74	1.72	1.70
14.61	15.30	15.10	15.13	15.07	14.93
4.15	2.90	3.90	3.14	3.97	3.52
5.83	7.28	6.29	7.24	6.38	6.67
0.17	0.17	0.19	0.19	0.16	0.18
7.40	7.28	7.21	7.29	7.67	7.69
10.83	11.14	11.10	11.19	11.02	10.87
2.89	2.82	2.90	2.84	2.85	2.88
0.22	0.22	0.31	0.18	0.22	0.26
0.14	0.15	0.17	0.17	0.16	0.15
0.004	0.08	0.02	0.09	0.05	0.07
2.00	1.11	1.26	1.30	1.76	1.77
98.53	99.85	99.50	99.97	99.84	99.51
9.56	9.89	9.80	10.07	9.95	9.84
0.605	0.593	0.593	0.589	0.604	0.607
0.434	0.293	0.227	0.312	0.399	0.358
2.3	0.7	4.5	1.5	2.8	2.3
134	129	132	131	130	129
35	36	37	37	37	37
114	117	125	121	121	122
2.0	2.1	2.2	2.5	1.9	2.1

Most samples selected for analysis were relatively fresh, with total water contents usually less than 2 per cent and oxidation ratios mostly below 0.4. It is unlikely, therefore, that the major- or trace-element chemistry of these samples will have been significantly modified by seawater alteration. The mobile elements K, Rb, and S are notable exceptions. The effects of alteration on sulfur are especially pronounced, and there is a marked inverse correlation between the oxidation ratio and the sulfur content (Figure 3). It would appear from this relationship that unaltered samples should contain about 0.14 per cent sulfur, a

TABLE 1 – *Continued*

Sample (Interval in cm)	395A-52-2, 75-80	395A-56-3, 62-65	395A-57-1, 40-43	395A-59-1, 67-70	395A-60-1, 66-70
JSC No.	153	154	155	156	157
Depth (m)	534	565	570	590	599
Basalt type	A_3	A_3	A_4	A_4	A_4
SiO_2	50.3	49.4	48.8	48.3	48.4
TiO_2	1.73	1.75	1.57	1.58	1.59
Al_2O_3	15.22	14.99	14.93	14.93	15.12
Fe_2O_3	2.94	3.21	2.32	2.69	3.21
FeO	7.37	7.12	8.02	7.65	6.94
MnO	0.19	0.18	0.19	0.16	0.19
MgO	7.34	7.82	8.62	8.45	8.01
CaO	11.10	10.82	10.55	10.71	10.77
Na_2O	2.76	2.80	2.80	2.83	2.85
K_2O	0.19	0.19	0.15	0.13	0.14
P_2O_5	0.16	0.18	0.15	0.13	0.12
S	0.11	0.07	0.09	0.05	0.07
Total H_2O	1.38	1.44	1.50	1.84	1.95
Total	100.75	100.02	99.51	99.42	99.36
Total Fe as FeO	10.02	10.01	10.11	10.07	9.83
Mg'-value	0.592	0.607	0.628	0.624	0.617
O. R.	0.293	0.321	0.229	0.267	0.326
Trace Elements (ppm)					
Rb	1.0	1.2	0.9	0.6	0.9
Sr	128	127	121	125	125
Y	37	38	34	34	35
Zr	119	125	107	109	109
Nb	2.8	2.7	2.4	2.4	1.8

Sample (Interval in cm)	395A-64-4, 130-135	395A-64, CC, 17-21	395A-66-1, 36-41	395A-66-3, 12-16	395A-67, CC, 130-135
JSC No.	164	165	166	167	168
Depth (m)	631	632	645	648	657
Basalt type	A_4	A_4	A_4	A_4	A_5
SiO_2	47.1	48.8	48.1	47.7	48.2
TiO_2	1.59	1.56	1.61	1.59	1.57
Al_2O_3	15.00	15.07	15.02	14.76	14.87
Fe_2O_3	5.07	3.90	3.84	4.71	2.48
FeO	5.49	6.36	6.63	5.87	7.86
MnO	0.19	0.17	0.18	0.21	0.18
MgO	7.72	8.15	8.32	7.99	8.57
CaO	10.67	10.77	10.77	10.67	10.85
Na_2O	2.96	2.76	2.77	2.96	2.69
K_2O	0.15	0.17	0.12	0.18	0.22
P_2O_5	0.13	0.13	0.14	0.14	0.15
S	0.00	0.08	0.05	0.00	0.08
Total H_2O	3.08	2.03	2.28	2.62	1.96
Total	99.13	99.94	99.83	99.37	99.72
Total Fe as FeO	10.05	9.87	10.09	10.11	10.09
Mg'-value	0.603	0.621	0.620	0.610	0.627
O. R.	0.505	0.395	0.381	0.466	0.246
Trace Elements (ppm)					
Rb	2.3	1.9	1.3	3.8	0.9
Sr	126	132	127	126	122
Y	35	33	36	35	34
Zr	108	107	112	109	107
Nb	2.7	1.8	2.0	2.5	1.4

value somewhat larger than that proposed by Moore and Fabbi (1971) as typical for unaltered basalts recovered from deep water.

Two broad basalt types, differing fundamentally in both petrography and whole-rock chemistry, prevail at Site 395. These are, respectively, the aphyric and phyric basalts. The aphyric basalts lack megascopic phenocrysts, but contain microphenocrysts of olivine and plagioclase; the phyric basalts contain abundant (10 to 30%) plagioclase phenocrysts, together with phenocrysts of olivine, rarer Cr-diopside, and minor chromian spinel. The aphyric basalts are the more

TABLE 1 – *Continued*

395A-60-3, 33-37	395A-61-1, 142-150	395A-62-1, 10-15	395A-63-1, 42-47	395A-63-4, 86-93	395A-64-1, 29-37
158	159	160	161	162	163
602	608	617	619	624	626
A_4	P_4'	P_4'	P_4'	P_4'	P_4'
47.2	49.2	49.3	49.6	48.5	49.1
1.55	1.21	1.09	1.12	1.06	1.06
15.09	16.05	17.15	16.47	17.19	17.21
5.02	3.81	2.10	2.68	3.92	3.27
5.36	4.92	5.93	5.56	4.16	4.71
0.18	0.15	0.16	0.17	0.15	0.16
8.40	7.84	7.93	8.18	7.56	7.31
10.60	11.71	11.63	11.59	11.77	12.45
2.77	2.72	2.70	2.54	2.64	4.21
0.16	0.16	0.08	0.09	0.12	0.10
0.13	0.10	0.08	0.09	0.09	0.08
0.01	0.01	0.11	0.05	0.00	0.02
2.17	1.66	1.75	1.78	2.75	1.31
98.61	99.55	100.02	99.92	99.90	100.87
9.88	8.35	7.82	7.97	7.69	7.65
0.627	0.650	0.668	0.670	0.661	0.654
0.508	0.456	0.269	0.336	0.510	0.427
2.2	3.9	0.8	1.0	4.0	1.7
117	128	122	123	130	136
34	27	23	24	22	23
103	78	69	71	65	68
2.3	0.6	1.1	0.3	0.8	0.9

TABLE 2
Chemical Composition of Basalt From Site 396

Sample (Interval in cm)	15-1, 110-115	16-1, 97-101	18-3, 147-150	22-2, 120-128	23-1, 58-61	24-2, 49-54	25-1, 134-139
JSC No.	173	176	175	171	172	169	170
Depth (m)	127	137	159	193	201	211	221
SiO_2	49.30	48.79	49.27	48.99	49.17	49.81	49.30
TiO_2	1.27	1.26	1.29	1.23	1.25	1.30	1.29
Al_2O_3	16.95	16.86	16.30	16.69	17.29	16.52	16.21
Fe_2O_3	1.39	3.64	3.85	3.65	4.33	3.92	4.43
FeO	7.15	4.90	4.72	4.68	4.19	5.02	4.68
MnO	0.17	0.15	0.14	0.14	0.13	0.17	0.17
MgO	7.48	8.03	7.66	7.60	6.42	7.21	6.86
CaO	11.80	11.85	11.48	11.66	12.07	11.76	11.69
Na_2O	2.66	2.87	2.75	2.79	2.77	2.72	2.68
K_2O	0.20	0.21	0.23	0.24	0.20	0.23	0.25
P_2O_5	0.09	0.08	0.08	0.09	0.09	0.09	0.15
S	0.05	0.05	0.02	0.02	0.02	0.01	0.03
Total H_2O	1.49	1.52	2.28	2.47	2.86	2.10	2.52
Total	100.00	100.21	100.70	100.24	100.79	100.86	100.26
Total Fe as FeO	8.40	8.17	8.18	7.96	8.09	8.55	8.68
Mg'-value	0.638	0.661	0.650	0.654	0.611	0.626	0.610
O.R.	0.165	0.445	0.471	0.459	0.535	0.459	0.510
Trace Elements (ppm)							
Rb	1.0	2.5	2.7	3.3	2.9	3.5	
Sr	149	145	160	145	152	127	
Y	26	27	28	26	27	28	
Zr	84	85	87	83	79	83	
Nb	2.1	1.4	1.6	2.0	1.1	1.4	

abundant, and comprise about 59 per cent of the cored interval.

Chemically, the phyric basalts are distinguished from the aphyric basalts by higher Al_2O_3 (16.5 to 19.2%) and CaO (11.5 to 12.8%) concentrations, and by lower SiO_2, FeO, and MgO concentrations (Figures 4 and 5). These differences are reflected in higher normative plagioclase contents and in lower Ab/(Ab+An) ratios in the phyric basalts. Although both total iron and MgO are lower in the phyric basalts,

TABLE 3
Trace Element Abundances (ppm) in Selected Leg 45 Samples

Sample (Interval in cm)	395-11-1, 42-44	395-11-2, 100-105	395-19-1, 57-62	395A-4-1, 66-69	395A-8-1, 70-73	395A-10-1, 144-146
JSC No.	109	111	116	117	120	123
Depth (m)	95	101	173	99	129	153
Basalt type	A_2	A_2	P_2	A_3	A_2	A_2
Sc	36.6	36.0	29.8	38.4	37.9	37.1
Cr	290	290	252	320	300	300
Ni	120	190	110	140	140	150
La	2.91	2.79	2.71	3.77	3.18	3.31
Ce	9.6	9.7	9.3	12.2	11.1	9.8
Sm	3.38	3.41	3.09	3.91	3.72	3.68
Eu	1.33	1.27	1.06	1.40	1.39	1.34
Tb	0.92	0.92	0.76	1.0	0.95	0.95
Yb	3.3	3.2	2.8	3.5	3.6	3.7
Lu	0.50	0.47	0.42	0.53	0.52	0.56
Hf	3.0	2.7	2.3	3.0	3.0	2.9

Sample (Interval in cm)	395A-25-1, 96-100	395A-27-2, 111-116	395A-31-1, 96-107	395A-34-1, 140-143	395A-41-1, 107-111	395A-49-1, 26-31
JSC No.	136	138	142	144	148	150
Depth (m)	285	306	339	372	433	504
Basalt type	P_4	P_4	P_5	A_3	A_3	A_3
Sc	33.8	33.5	32.3	38.5	38.7	38.8
Cr	340	340	310	280	290	290
Ni	150	130	140	110	100	40
La	2.41	2.33	2.48	3.82	3.70	4.14
Ce	8.1	7.2	8.1	11.7	12.3	12.5
Sm	2.77	2.72	2.82	4.10	4.09	4.28
Eu	1.06	1.04	1.06	1.43	1.47	1.45
Tb	0.72	0.60	0.67	0.99	1.05	1.09
Yb	2.5	2.7	2.7	3.7	3.6	3.8
Lu	0.40	0.40	0.41	0.56	0.55	0.56
Hf	2.3	2.2	2.2	3.3	3.3	3.2

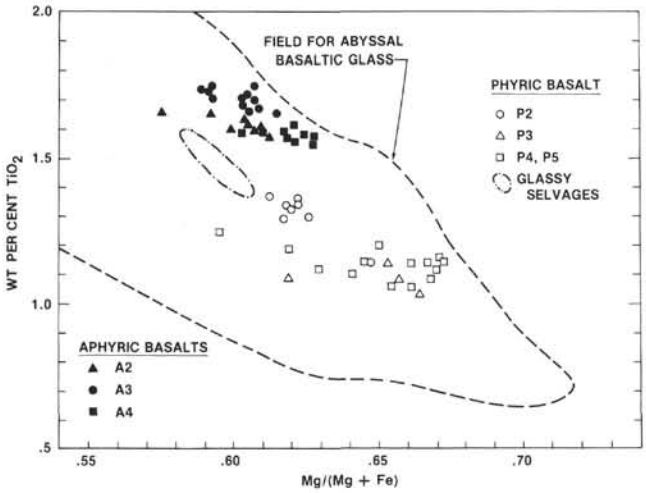

Figure 2. *TiO_2 versus Mg′-value for Leg 45 basalts. The field for abyssal volcanic glass compositions is taken from the data of Melson et al. (1976).*

Mg′-values tend to be higher, an indication that they are more "primitive" than the aphyric basalts (Figures 2 and 5). TiO_2, and most other minor- and magmaphile trace-element abundances are markedly lower in the phyric basalts (Figure 2). This difference extends also to the glassy rims of the phyric basalts, and is therefore not simply a consequence of plagioclase dilution. Strontium, on the other hand, is higher in the phyric

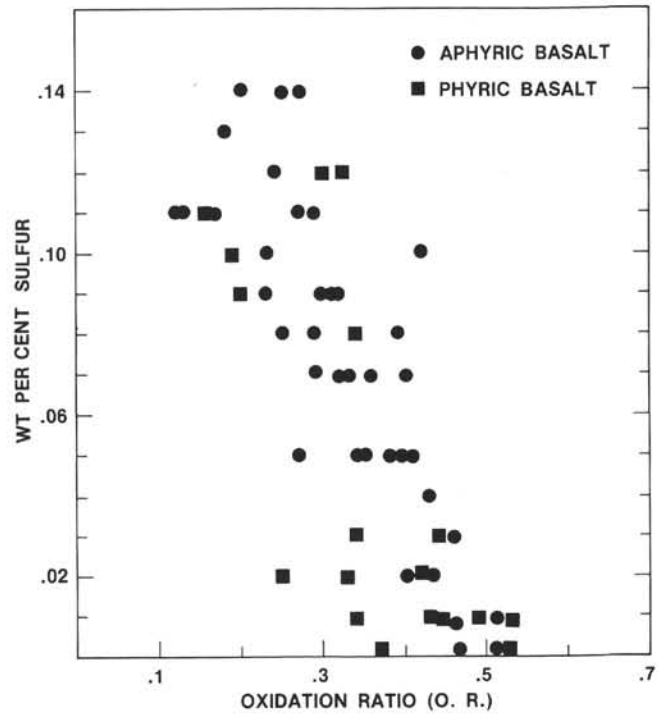

Figure 3. *Relationship of sulfur content to oxidation ratio (O.R.) in Leg 45 basalts. The juvenile sulfur content of the basalts is inferred to have been greater than 0.14 per cent.*

TABLE 3 – *Continued*

395A-14-2, 140-147	395A-15-4, 10-15	395A-15-4, 16-20	395A-15-5, 16-20	395A-15-5, 16-20	395A-19-1, 132-136	395A-21-1, 87-90
125	128(1)	128(2)	130	130	132	133
186	199	199	201	201	231	244
P_2	P_2	P_2	P_2	P_2	P_3	P_3
31.1	31.5	32.6	28.2	29.0	32.5	32.4
220	290	250	260	300	377	380
87	83	90	100	70	110	130
2.93	2.79	2.95	2.42	2.40	2.02	2.07
9.5	9.2	9.7	8.0	7.8	6.7	6.8
3.20	3.05	3.26	2.66	2.68	2.38	2.45
1.17	1.16	1.20	1.01	1.03	0.91	0.93
0.82	0.71	0.76	0.64	0.69	0.66	0.62
3.0	2.7	2.8	2.4	2.4	2.4	2.4
0.45	0.42	0.46	0.37	0.36	0.36	0.37
2.4	2.4	2.6	2.1	1.9	1.9	1.9

	395A-56-3, 62-65	395A-57-1, 40-43	395A-61-1, 142-150	395A-63-4, 86-93	395A-66-1, 36-41	395A-67-CC, 130-135
153	154	155	159	162	166	168
539	567	573	609	626	645	660
A_3	A_3	A_4	P_4	P_4	A_4	A_4
37.8	38.3	36.7	35.6	30.6	36.7	36.6
280	260	340	320	380	320	330
120	120	170	110	140	140	140
3.81	4.24	3.34	2.24	2.30	3.18	3.37
12.1	12.6	10.4	8.2	8.4	10.3	10.6
4.33	4.20	3.67	2.81	2.93	3.56	3.67
1.36	1.51	1.34	1.08	1.08	1.39	1.33
1.02	1.06	0.93	0.72	0.72	0.99	0.94
3.9	3.9	3.3	2.5	2.6	3.2	3.6
0.59	0.58	0.53	0.38	0.43	0.47	0.50
3.2	3.2	3.1	2.2	2.4	2.8	3.3

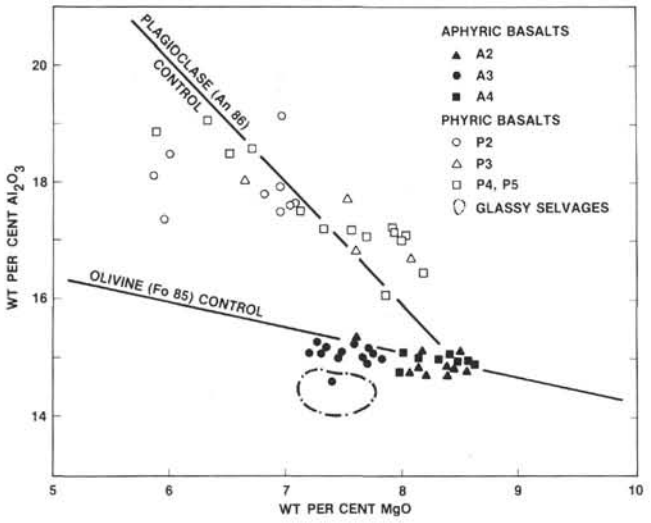

Figure 4. *Al_2O_3 versus MgO for Leg 45 basalts. The olivine and plagioclase control lines are for illustrative purposes only; they are not intended as lines of "best fit," or to imply that the basalts are related simply by olivine and plagioclase fractionation.*

basalts, both in absolute terms and with respect to other magmaphile elements. Consequently, Sr/Zr ratios are distinctly different in the two basalt types, and vary widely in the phyric basalts (1.55 to 2.46), in contrast to the lower, essentially constant values (1.02 to 1.18) in the aphyric basalts.

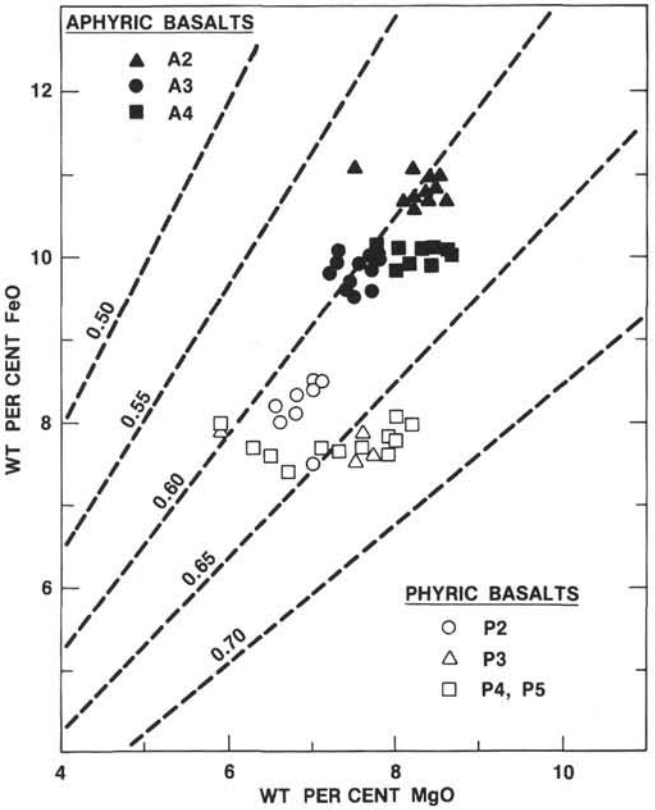

Figure 5. *MgO-FeO relationships for Leg 45 basalts. The dashed lines indicate Mg'-values from 0.5 to 0.7.*

Figure 1 illustrates the normative olivine, plagioclase, and pyroxene relationships for these basalts, relative to the inferred olivine-plagioclase cotectic of Shido et al. (1971). All the aphyric basalts plot in the olivine tholeiite field, within a tightly controlled elongate group sub-parallel to the inferred cotectic. In contrast, the phyric basalts plot predominantly within the plagioclase tholeiite field and are widely scattered. Those phyric basalts plotting close to the inferred cotectic, or just within the olivine tholeiite field, have the lowest Al_2O_3 contents. Presumably, they contain fewer plagioclase phenocrysts than the majority of samples, and may be closer to melt compositions. As might be expected from these relationships, in a one-atmosphere melting experiment on a typical phyric basalt (#138), plagioclase is the first phase to crystallize, followed by olivine, whereas in a typical aphyric basalt (#122), olivine is the liquidus phase, followed by plagioclase (Dungan et al., this volume).

Initial studies, based on shipboard X-ray fluorescence analyses, recognized within the two major basalt types 10 compositionally distinct magmatic units. These are, in order of increasing depth below the sediment/basement interface, A1, A2, P1, P2, P3, P4, P5, A3, A4, P4, A4, and A5, where A denotes aphyric basalt and P phyric basalt.

Our data essentially confirm these subdivisions, subject to minor revisions in light of the more recent and comprehensive data. Average values, calculated from the data in Table 1, are given in Table 4. In order of increasing depth within Hole 395A, the compositional units following can be identified.

TABLE 4
Average Compositions of Leg 45 Basalt Types

	Aphyric Basalts			Phyric Basalts				
	A2	A3	A4	P2	P3	P4	P4 Sill	P5
Major Elements (wt %)								
SiO_2	48.96	49.28	48.07	49.16	49.27	49.22	49.15	49.13
TiO_2	1.61	1.71	1.58	1.31	1.07	1.16	1.11	1.14
Al_2O_3	14.90	15.07	14.98	17.98	17.54	17.77	16.81	18.08
FeO*	10.81	9.84	10.01	8.11	7.85	7.71	7.90	7.74
MnO	0.19	0.18	0.18	0.14	0.14	0.15	0.16	0.14
MgO	8.27	7.48	8.36	6.75	7.27	7.20	7.76	7.03
CaO	10.28	11.03	10.71	11.68	12.50	12.22	11.83	12.07
Na_2O	2.89	2.85	2.82	2.78	2.40	2.70	2.65	2.75
K_2O	0.15	0.23	0.16	0.10	0.13	0.15	0.11	0.16
P_2O_5	0.13	0.16	0.13	0.11	0.09	0.11	0.09	0.10
S	0.11	0.06	0.04	0.09	0.02	0.01	0.04	0.02
Mg′-value	0.602	0.601	0.623	0.622	0.647	0.649	0.661	0.643
Trace Elements (ppm)								
Rb	1.4	2.3	1.6	0.9	1.9	2.0	2.3	2.5
Sr	116	130	125	154	114	139	129	154
Y	34.9	36.5	34.4	27.7	23.0	24.8	23.8	24.5
Zr	105	119	108	88	63	74	70	75
Nb	1.9	2.2	2.1	1.5	1.2	1.2	0.7	1.1
La	3.05	3.94	3.30	2.70	2.05	2.37	2.27	2.48
Ce	10.1	12.2	10.4	8.9	6.7	7.7	8.3	8.1
Sm	3.55	4.20	3.63	2.99	2.42	2.75	2.87	2.82
Eu	1.33	1.44	1.35	1.11	0.92	1.05	1.08	1.06
Tb	0.94	1.04	0.95	0.73	0.64	0.76	0.72	0.67
Yb	3.5	3.8	3.4	2.7	2.4	2.6	2.5	2.7
Lu	0.51	0.57	0.50	0.41	0.36	0.40	0.40	0.41
Hf	2.9	3.2	3.1	2.3	1.9	2.3	2.3	2.2
Sc	36.9	38.4	36.7	30.4	32.5	33.7	33.1	32.3
Cr	295	280	330	262	379	340	350	310
Ni	150	98	150	90	120	140	125	140
La/Sm	0.86	0.94	0.91	0.90	0.85	0.86	0.79	0.88
La/Yb	0.87	1.04	0.97	1.00	0.85	0.91	0.91	0.92
Sm/Eu	2.67	2.92	2.69	2.69	2.63	2.62	2.66	2.66
Sr/Zr	1.10	1.09	1.16	1.75	1.81	1.88	1.84	2.05
Zr/Nb	55	54	51	59	53	62	100	68
Zr/Y	3.01	3.26	3.14	3.2	2.7	3.0	2.9	3.1
Ti/Zr	92	86	88	89	102	94	95	91
Zr/Hf	36	37	35	38	33	32	30	34

Aphyric Unit A2 (106 to 173 m)—This is the uppermost aphyric unit, and occurs in the upper 29 meters of Hole 395, as well as in Hole 395A. It consists of a thick sequence of chemically homogeneous, rapidly chilled pillow basalts, and has a characteristic variolitic texture containing microphenocrysts of olivine. This basalt type is distinguished from the other aphyric basalts principally on the basis of higher iron concentrations (10.6 to 11.1%) and by slightly lower abundances of strontium (Table 4). The compositional variation is small, and is commensurate with minor (<5%) olivine fractionation.

In the initial shipboard studies, the magmatic Unit A1 was based on a single sample (11-1, 103-108 cm) from near the top of basement in Hole 395. It was more iron-rich than underlying members of the A2 basalts. In order to locate the A1/A2 boundary we have analyzed basalts immediately above and below this sample, and find that they have typical A2 compositions (Table 1, #109, 110). From this we conclude that Unit A1 is not a distinct magmatic unit, and that the iron-rich sample analyzed during shipboard studies is a more evolved variant of the A2 basalt type.

Phyric Unit P2 (173 to 201 m)—This unit occurs at the top of the thick 181-meter sequence of phyric basalts that were cored in Hole 395A, and also occurs in the bottom 10 meters of Hole 395. In Hole 395A, almost all of this unit is composed of a single thick (25 m), massive cooling unit. Except for the lowermost sample in the cooling unit (Table 1, #130), the P2 basalts are uniform in composition, and are more evolved than the other phyric basalts. This is reflected in lower Mg′-values and higher abundances to TiO_2 and other magmaphile elements (Figure 2). The lowermost sample in the cooling unit is higher in Al_2O_3, has a higher Mg′-value, and has correspondingly lower abundances of magmaphile elements. In many respects it resembles other, more "primitive" phyric basalts lower in the stratigraphic sequence. We attribute this difference to either preferential accumulation of plagioclase and olivine phenocrysts at the base of the cooling unit, or upward migration of interstitial magma, caused by filter pressing.

Phyric Unit P3 (201 to 260 m)—This unit is distinguished from the other phyric units by lower TiO_2 and magmaphile element abundances (Figures 2 and 6). Strontium is also low in this unit (110 to 119 ppm), relative to all other phyric basalts. The plagioclase-olivine phyric basalt associated with the brecciated serpentinized periodotite zone in Hole 395 is also low in strontium (Table 1, #115), and tends to be lower in magmaphile elements than most other phyric basalts. In many respects, it closely resembles the P3 basalt type in Hole 395A, and may simply be fragments of this basalt type incorporated into the breccia zone, rather than a separate magmatic unit (P1) as was suggested by the shipboard studies.

Phyric Units P4 and P5 (260 to 356 m)—Initial shipboard analyses indicated that these two basalt types are essentially similar in bulk chemistry, but

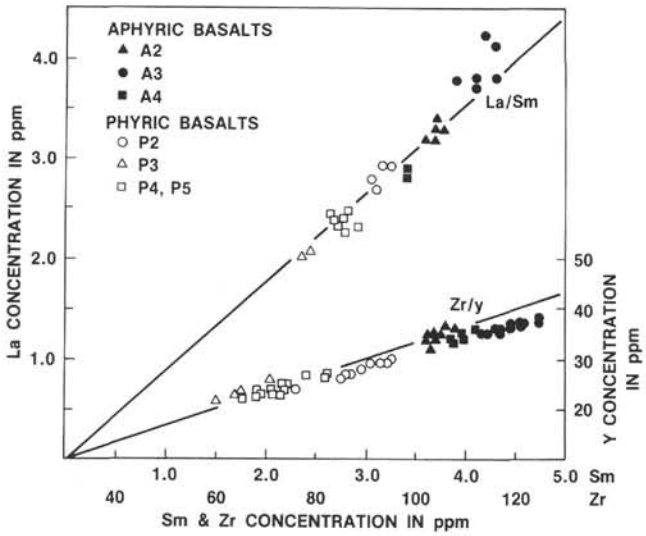

Figure 6. *Lanthanum-Samarium and Zirconium-Yttrium relationships in Leg 45 basalts. The lines shown are for constant La/Sm and Zr/Y ratios.*

differ in strontium content. Additional analyses reported here (Table 1) show that both units contain strontium in a wide range of values: strontium in P4 varies between 122 and 165 ppm, and in P5 between 132 and 175 ppm. Consequently, we believe that the initial distinction between these two basalt types is no longer tenable.

As a group these basalts are highly variable both in Al_2O_3 content, which varies from 16.1 to 19.1 per cent, and in Mg′-values (between 0.59 and 0.67 per cent). Much of this variability must be attributed to localized variation in plagioclase and olivine phenocryst content.

Deeper in the section (608 to 629 m), there is a massive (21 m) cooling unit chemically equivalent to the P4-P5 phyric basalts. We believe this to be a sill that intruded underlying aphyric basalts penecontemporaneously with extrusion of the P4-P5 basalts.

Aphyric Unit A3 (356 to 570 m)—This exceptionally thick sequence of compositionally uniform pillow basalts is more evolved than the other aphyric units. These basalts are multiply saturated with microphenocrysts of both olivine and plagioclase (Dungan et al., this volume), and plot towards the low-temperature end of the inferred cotectic in Figure 1. Although the Mg′-values compare closely with those of the A2 basalts (e.g., 0.59 to 0.61), they are distinctly lower in both FeO and MgO (Figure 5), and on the basis of fig. 7 in Roeder and Emslie (1970), can be inferred to have lower liquidus temperatures. In keeping with their evolved nature, these basalts have the highest lithophile element abundances, and are characterized by a more distinct Eu anomaly than is observed for the other aphyric basalts. The unit as a whole exhibits little compositional variation, and there are no obvious fractionation trends.

At the sediment/basement interface in Hole 395A is a rubble zone containing fragments of aphyric basalt, serpentinized peridotite, and gabbro (Cores 4 and 5). Two of these basalts are indistinguishable from the A3 basalts (Table 1, # 117, 118); this suggests that this basalt type is exposed at the surface of the basement within close proximity to the drill site.

Aphyric Unit A4 (570 to 608 m and 629 to 657 m)—This unit is intruded by a 21-meter sill compositionally equivalent to the P4-P5 phyric basalts. There is no appreciable difference in chemistry between the basalts above the sill (Table 1, #155-160) and those beneath (Table 1, #161-168). All are aphyric basalts containing olivine microphenocrysts. They are both texturally and chemically similar to the A2 basalts, but can be distinguished from them by a tendency toward higher normative olivine contents (Figure 1), higher Mg′-values (0.60 to 0.63), and lower total iron concentrations for a given value of MgO (Figure 5). TiO_2, Sr, and the magmaphile element abundances are essentially identical to those of the A2 basalts.

DISCUSSION

The chondrite-normalized rare-earth abundances for the Leg 45 samples (Figure 7) show them to be "normal" LIL-element-depleted basalts. They are light-rare-earth depleted, and have La/Sm and La/Yb ratios less than 1.0 (Table 4), similar to the Type I basalts of Bryan et al., (1976). The Nb content of these basalts is low, resulting in high Zr/Nb ratios (mean = 58) similar to those in other LIL-element-depleted basalts (Pearce and Cann, 1973; Erlank and Kable 1976; Rhodes et al., 1976), and considerably higher than the Zr/Nb ratios (<10) of oceanic islands and "anomalous" Type II basalts sampled on the Mid-Atlantic Ridge at 45°N and in the FAMOUS area (Erlank and Kable, 1976; Rhodes et al., unpublished data). Two $^{87}Sr/^{86}Sr$ values of 0.70276 ± 10 and 0.70280 ± 8, obtained for Samples 117 and 153, respectively, are also characteristic of "normal," Type I LIL-element-depleted basalts (Hart, 1976).

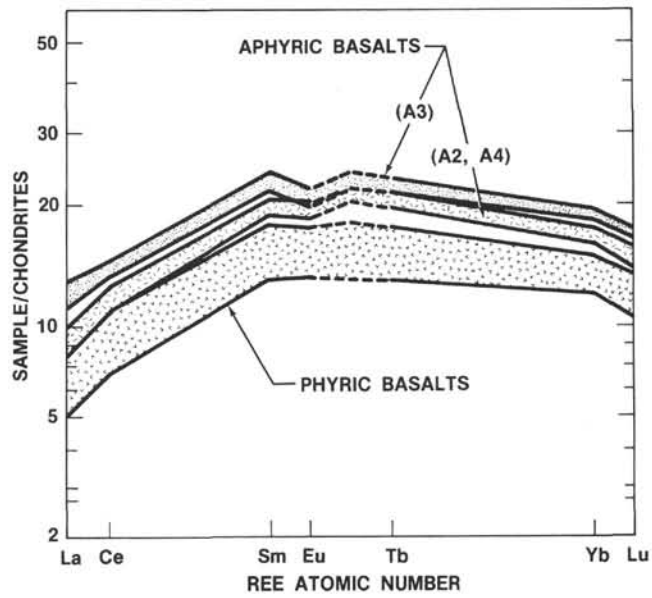

Figure 7. *Chrondite-normalized abundances in Leg 45 basalts.*

Inspection of Figures 6 and 7 and Table 4 shows that most magmaphile element ratios are very similar for the various basalt types, and do not differ substantially between the phyric and aphyric basalts. An obvious exception is the ratio of strontium to other magmaphile elements. This is illustrated by the Sr/Zr ratio, which is constant in the aphyric basalts, where Sr behaves as a magmaphile element, but is both distinctly different and highly variable in the phyric basalts, where plagioclase influence is prevalent. Since many magmaphile element ratios and the characteristic REE patterns are not substantially changed by fractional crystallization involving the observed phenocryst phases, olivine, and plagioclase (Kay et al., 1970; Schilling 1971; Frey et al., 1974; Schilling, 1975), we deduce that these ratios reflect the characteristics of the mantle source region, and that all of the various basalt types were derived from an essentially similar and homogeneous LIL-element-depleted mantle source. Similar ratios pertain to basalts from Holes 396 (Table 2) and 396B (Dungan et al., *Initial Reports of the Deep Sea Drilling Project*, v. 46, in preparation); this implies a widespread and homogeneous mantle source for basaltic vulcanism along this section of the Mid-Atlantic Ridge. This contrasts markedly with the wide variations in magmaphile element ratios found in Leg 37 basalts, both within and between holes (Blanchard et al., 1976), and the consequent necessity to postulate a complex and heterogeneous mantle source for the basalts in that region.

Although these basalts appear ultimately to have been derived by partial melting of a common source, all are evolved and have undergone moderate amounts of differentiation. Evidence of this is provided by the low Mg′-values (0.57 to 0.67), low Ni concentrations (<190 ppm), moderate magmaphile element abundances (e.g., TiO_2 = 1.0 to 1.7%), and the presence of multiple phenocryst phases in all but the A2 and A4 basalts. Since the compositional variation within the individual basalt groups is small, and there are no clearly defined internal fractionation trends, we suggest that magma compositions were established by differentiation within shallow magma chambers, followed by episodic eruption onto the sea floor, with little or no fractionation at the surface or enroute to the surface.

There can be little doubt that the compositions of the glassy and variolitic aphyric basalts are close to those of magmatic liquids. The compositions of the phyric basalts are more enigmatic. Several lines of evidence indicate that these rocks are far removed from liquid compositions: (a) Compilations of basaltic glass compositions (Melson et al., 1976) indicate that magmatic liquids with more than 17 per cent Al_2O_3 are extremely rare. Similarly, the glassy selvages on the phyric basalts (unpublished data) are much lower in Al_2O_3 and not substantially different from the aphyric basalts (Figure 4). (b) The wide scatter of compositions in the normative olivine-plagioclase-pyroxene diagram (Figure 1) suggests plagioclase and olivine addition to liquids close to the inferred olivine-plagioclase cotectic. Plagioclase addition trends are also evident in several other variation diagrams (e.g., Figures 4 and 5). (c) Dungan et al. (this volume) present experimental, textural, and compositional evidence indicating that many of the plagioclase and olivine phenocrysts are too anorthitic or forsteritic to have crystallized from melts having the compositions of the phyric basalts, but derive instead from more "primitive" basalts.

From this evidence, we think that the phyric basalts have a mixed heritage, resulting from mixing of consanguineous "primitive" and evolved magmas and their attendant phenocrysts. If this interpretation is correct, the higher Mg′-values, normative An/(Ab+An) ratios, and lower magmaphile element abundances of the phyric basalts relative to the aphyric ones result in part from the addition of up to 20 per cent plagioclase and 5 per cent olivine phenocrysts. The glassy rims on phyric basalt pillows probably provide the most reliable estimate of the melt compositions. They have Mg′-values comparable to those of the more evolved aphyric basalts (<0.60), but are distinguished from them by lower TiO_2 values (Figure 2) and by higher CaO/Al_2O_3 ratios. Thus, the phyric basalts are not simply related to any of the aphyric basalts types by processes of plagioclase and olivine accumulation.

An understanding of the relationships between the various phyric basalt units is also frustrated by uncertainty concerning melt compositions. In terms of increasing magmaphile element abundances, the basalt types are ranked as follows: P3, P4-5, P2. This is not simply a function of decreasing plagioclase and olivine accumulation, but reflects a fundamental property of each of the basalt types. The increase in magmaphile element abundances from P3 to P2 is too large and varied, however, to be accounted for simply by crystal fractionation of the dominant phenocryst phases, plagioclase and olivine, and cannot readily be reconciled with the absence of systematic changes in major element chemistry. We attribute these differences in the magmaphile element abundances in the phyric basalts to discrete magma types, containing varying proportions of admixed plagioclase, olivine, and rarer clinopyroxene phenocrysts.

The relationships between the three aphyric basalt units are less complicated. The A2 and A4 basalts are broadly similar in major- and trace-element chemistry, and both contain only olivine as the microphenocryst phase. The A2 basalts are higher in total iron and tend to have lower Mg′-values than the majority of the A4 basalts (Figure 5). Consequently, these two basalt types cannot be related by olivine fractionation, the only observed phenocryst phase, and the liquidus phase in equilibrium melting experiments (Dungan et al., this volume). The A3 basalts contain microphenocrysts of both olivine and plagioclase, and are more evolved than the stratigraphically lower A4 basalts, from which they may have been derived by olivine fractionation. The magmaphile element abundances,

however, are at variance with this interpretation. Some elements, such as Sr, Y, and Sc are increased in the A3 basalts relative to the A4 basalts, commensurate with the 5 per cent olivine and plagioclase fractionation required by the major-element data. The differences in other elements (e.g., Ti, Zr, La, Sm, Yb) are, however, too large to have resulted from such a small amount of fractionation. Further, the amount of fractionation estimated from the reciprocal of the ratio of magmaphile elements in the A3 to the A4 basalts (Anderson and Greenland, 1969) is not constant for the different elements, and varies from as little as 4 per cent for Sr to as much as 20 per cent for Sm. Clearly, these magma types are not related directly by crystal fractionation processes.

CONCLUSION

We have, at the Leg 45 site, several discrete magma types, both phyric and aphyric, not related directly by crystal fractionation, which appear to have been derived from a common mantle source. The prevailing interpretation of such relationships is that each basalt type represents an evolved derivative of more "primitive" basaltic magmas, resulting from varying degrees of melting of a common mantle source. The evidence presented here, of magma mixing in the phyric basalts, suggests that such an interpretation may be too simple. We suggest instead that magma mixing of consanguineous evolved and "primitive" basalts, together with their attendant phenocrysts, may better explain many characteristics of the basalts. A subsequent publication documenting the role of magma mixing in these and other ocean floor basalts is in preparation (Rhodes et al., in press).

REFERENCES

Anderson, A. T. and Greenland, L. P., 1969. Phosphorus fractionation diagram as a quantitative indicator of crystallization differentiation of basaltic liquids, *Geochim. Cosmochim. Acta*, v. 33, p. 493-505.

Bass, M. N., 1971. Variable abyssal basalt populations and their relation to sea-floor spreading rates, *Earth Planet. Sci. Lett.*, v. 11, p. 18-22.

Blanchard, D. P., Rhodes, J. M., Dungan, M. A., Rodgers, K. V., Donaldson, C. H., Brannon, J. C., Jacobs, J. W., and Gibson, E. K., 1976. The chemistry and petrology of basalts from Leg 37 of the Deep Sea Drilling Project, *J. Geophys. Res.*, v. 81, p. 4231-4246.

Bryan, W. B. and Moore, J. G., 1976. Compositional variations of young basalts in the Mid-Atlantic Ridge rift valley near lat. 46°49′N, *Geol. Soc. Am. Bull.*, v. 88, p. 556-570.

Bryan, W. B., Thompson, G., Frey, F. A., and Dickey, J. J., 1976. Inferred settings and differentiation in basalts from the Deep Sea Drilling Project, *J. Geophys. Res.*, v. 81, p. 4285-4304.

Engel, A. E., Engel, C. G., and Havens, R. G., 1965. Chemical characteristics of oceanic basalts and the upper mantle, *Geol. Soc. Am. Bull.*, v. 76, p. 719-734.

Erlank, A. J. and Kable, E. J. D., 1976. The significance of incompatible elements in Mid-Atlantic Ridge basalts from 45°N, with particular reference to Zr/Nb, *Contrib. Mineral. Petrol.*, v. 54, p. 281-291.

Frey, F. A., Bryan, W. B., and Thompson, G., 1974. Atlantic ocean floor: Geochemistry and petrology of basalts from Legs 2 and 3 of the Deep Sea Drilling Project, *J. Geophys. Res.*, v. 79, p. 5507-5527.

Hart, S. R., 1976. LIL-element geochemistry, Leg 34 basalts. *In* Hart, S. R., Yeats, R. S., et al., *Initial Reports of the Deep Sea Drilling Project*, v. 34: Washington (U.S. Government Printing Office), p. 283-288.

Jacobs, J. W., Korotev, R. L., Blanchard, D. P., and Haskin, L. A., in press. A well tested procedure for instrumental neutron activation analysis of silicate rocks and minerals, *J. Radioanal. Chem.*

Kay, R., Hubbard, N. J., and Gast, P. W., 1970. Chemical characteristics and origin of oceanic ridge volcanic rocks, *J. Geophys. Res.*, v. 75, p. 1585-1613.

Maxwell, J. A., 1968. *Rock and mineral analysis:* New York (Interscience), p. 419-421.

Melson, W. G., Vallier, T. L., Wright, T. L., Byerly, G., and Nelen, J., 1976. Chemical diversity of abyssal volcanic glass erupted along Pacific, Atlantic, and Indian ocean sea-floor spreading centers. *In The geophysics of the pacific ocean basin and its margin*: Washington (American Geophysical Union), p. 351-367.

Moore, J. G. and Fabbi, B. P., 1971. An estimate of the juvenile sulfur content of basalt, *Contrib. Mineral. Petrol.*, v. 33, p. 118-127.

Norrish, K. and Chappell, B. W. 1967. X-ray fluorescence spectrography. *In* Zussman, J. (Ed.), *Physical methods in determinative mineralogy*: New York (Academic Press), p. 161-214.

Norrish, K. and Hutton, J. T., 1969. An accurate X-ray spectrographic method for the analysis of a wide range of geological samples, *Geochim. Cosmochim. Acta*, v. 33, p. 431-453.

Pearce, J. A., and Cann, J. R., 1973. Tectonic setting of basic volcanic rocks determined using trace element analysis, *Earth Planet. Sci. Lett.*, v. 19. p. 290-300.

Reynolds, R. C., 1967. Estimation of mass absorption coefficients by Compton scattering: Improvements and extensions of the method, *Am. Mineralogist*, v. 48, p. 1133-1143.

Rhodes, J. M., Blanchard, D. P., Rodgers, K. V., Jacobs, J. W., and Brannon, J. C., 1976. Petrology and chemistry of basalts from the Nazca Plate: Part 2-major and trace element chemistry. *In* Hart, S. R., Yeats, R. S., et al., *Initial Reports of the Deep Sea Drilling Project*, v. 34: Washington, D. C. (U.S. Government Printing Office), p. 239-244.

Rhodes, J. M., Dungan, M. A., Blanchard, D. P. and Long, P. E., in press. Magma mixing at mid-ocean ridges: Evidence from basalts drilled near 22°N on the Mid-Atlantic Ridge, *Tectonophysics.*

Roeder, P. L. and Emslie, P. F., 1970. Olivine-liquid equilibrium, *Contrib. Mineral. Petrol.*, v. 29, p. 275-289.

Schilling, J. G., 1971. Sea-floor evolution: Rare-earth evidence, *Phil. Trans. Roy. Soc. London*, ser. A., v. 268, p. 663-706.

_____, 1975. Rare earth variations across 'normal segments' of the Reykjanes Ridge, 60°-53°N, Mid-Atlantic Ridge, 29°S, and East Pacific rise 2°-19°S, and evidence on the composition of the underlying low velocity layer, *J. Geophys. Res.*, v. 80, p. 1459-1473.

Shido, F. A., Miyashiro, A., and Ewing, M., 1971. Crystallization of abyssal tholeiites, *Contrib. Mineral. Petrol.*, v. 31, p. 251-266.

Yoder, H. S. and Tilley, C. E., 1962. Origin of basalt magmas: an experimental study of natural and synthetic rock systems, *J. Petrol.*, v. 3, p. 342-532.